

First principles calculations of zinc blende superlattices with ferromagnetic dopants

A. WRONKA*

Department of Solid State Physics, University of Łódź, Pomorska 149/153, 90-236 Łódź, Poland

Technological advances in device micro- and nano-fabrication over the past decade have enabled a variety of novel heterojunction device structures to be made in various spintronic device applications [1]. Among these, diluted and digital ferromagnetic half-metallic heterostructures and multilayers with ferromagnetic dopants exhibit a rich variety of features, with the potential for future generations of electronic devices with improved sensitivity and higher packing density. We investigate the electronic and magnetic structure of three-component Fe/MnAs/AsGa(0,0,1) thin superlattices in various supercell geometries. Calculations are performed by means of density functional theory (DFT) within the general gradient approximation with ultrasoft pseudopotentials, a plane-wave basis, and non-collinear magnetism. In our DFT calculations, we have found that the half-metallicity (HM) of MnAs/AsGa digital alloys can be destroyed by embedding Fe submonolayers.

Key words: *digital ferromagnetic heterostructure; density functional theory; half-metals*

1. Introduction

Ferromagnetic III–Mn–V semiconductors, such as (Ga, Mn)As random alloys, MnAs/GaAs digital alloys with Mn and GaAs layers grown alternately by molecular beam epitaxy, and zinc blende ferromagnetic heterostructures (FH) based on them are very promising candidates for materials that may be useful in spin electronic devices. There is evidence that the distance of spin diffusion in these semiconductors is long, with values of many microns being reported for GaAs. Mn-doped GaAs is a tetrahedrally bonded, half-metallic material that has been successfully used for spin-polarized injection into GaAs, III–V [2], and II–VI [3] semiconductors, opening the prospect of combining spin electronics and opto-electronics. Inspired by new possibilities of spin-dependent transport properties, the concept of a spin transistor has been put forward by Datta and Das [4], in which spin-polarized electrons are injected from a magnetic source, manipulated and controlled before they are collected at the mag-

*E-mail: awronka@uni.lodz.pl

netic drain. In these types of devices, not only the charge properties of the electrons are used, but also the fact that the electron has a spin degree of freedom.

The suggested applications include, e.g. “spin-field-effect-transistors” [4] which could allow software re-programming of microprocessor hardware during run-time, semiconductor-based “spin-valves” [5] which would result in high density, non-volatile semiconductor memory chips, and even “spin qubits” [6] to be used as basic building blocks for quantum computing.

Mn/GaAs superlattices [7] have remarkable properties in comparison to random (Ga,Mn) alloys. The Curie temperature of the alloy system is a linear function of Mn concentration, what can be described in the first approximation by the Zener model [8]. The solubility limit of Mn in GaAs is rather low, but large Mn concentrations, up to 50%, can be obtained in the MnAs/GaAs superlattice with MnAs submonolayers embedded into GaAs. The Curie temperature decays for increasing GaAs interlayer thickness for these structures, but saturates at thicknesses above ~ 50 GaAs monolayers (ML) [7], which is unexpected in the three dimensional Zener model and suggests that digital ferromagnetic heterostructures behave like planar systems [9] and magnetic interactions are confined to the MnAs layers. Theoretical *ab initio* calculations of thin superlattices of zinc blende compounds have been performed in the framework of density functional theory (DFT) by several authors [10, 11].

2. Method of calculation

In this paper, we intended to extend first-principle calculations to describe the magnetic moment distribution of a zinc blende multilayer and heterostructure with Mn and Fe dopants. Non-collinear magnetism and augmented plane wave (APW) methods [12], based on the total energy calculations implemented in the PWscf *ab initio* package [13], were used. The energies and atomic magnetic moments were calculated by total energy minimisation, using plane wave, Vanderbilt-type ultrasoft pseudopotentials (US-PPs) [14] as an approximation to the core-valence interaction based on DFT [15] in the general gradient approximation (GGA) [16]. Spin polarized calculations were carried out to account for different spin channels. A kinetic energy cut-off of 30 Ry was used for the plane waves included in the basis set. A $16 \times 16 \times 1$ Monkhorst-Pack [17] plane k -point mesh was used for the wave vector summation to the multilayer slab, and for the digital alloy MnAs/(GaAs) heterostructure a $8 \times 8 \times 6$ k -mesh was implemented. We used a supercell model, with a zinc blende (ZB) tetragonal unit cell with $a_0/(2)^{1/2}$ in the a and b directions. The GGA-optimised lattice constant of GaAs ($a_0 = 5.722$ Å) was used for all calculations. We have performed non-collinear magnetism calculations to evaluate the influence of the alloy electronic structure on the magnetization of ferromagnetic impurities (Mn and Fe monolayers).

We study the magnetic and electronic properties of zinc blende digital heterostructures with Mn and Fe planar impurities in DFT calculations. We consider three supercell geometries for DFT, with the relative atomic positions described in Table 1: a 14-atom super-

cell (1–14) for the Fe/Ga_{0.5}Mn_{0.5}As/AsGa/Ga_{0.5}Mn_{0.5}As/Fe multilayer (slab) with 3 AsGa ML of vacuum to isolate this supercell from others; a 13-atom supercell (2–14) for the heterostructure Ga_{0.5}Mn_{0.5}As/AsGa/Ga_{0.5}Mn_{0.5}As/Fe; a 12-atom supercell (2–13) for the heterostructure Ga_{0.5}Mn_{0.5}As/AsGa/Ga_{0.5}Mn_{0.5}As with no Fe submonolayers. By Ga_{0.5}Mn_{0.5}As we denote a 4-atom region of a GaAs unit with a MnAs monolayer. We use 0.5 ML, with Mn substituting Ga (because only 0.5 ML of Mn can be deposited by the MBE technique) and 0.5 ML of Fe atoms placed on As/Ga positions.

3. Results

In the first step, we obtained the atomic magnetic moment and electron charge distributions for the thin ZB superlattice and multilayer by means of non-collinear DFT calculations, as displayed in Table 1.

Table 1. The supercell relative atomic positions, magnetization distribution, and charge for the Fe/Ga_{0.5}Mn_{0.5}As/AsGa/Ga_{0.5}Mn_{0.5}As/Fe multilayer (upper values of magnetization and charge for atomic positions 1–14), and the Ga_{0.5}Mn_{0.5}As/AsGa/Ga_{0.5}Mn_{0.5}As/Fe superlattice (positions 2–14)

Atom number	Element	Relative position			Magnetization [μ_B]			Charge [a. u.]
		x	y	z	M_x	M_y	M_z	
1	Fe	0.0	0.0	-0.3536	1.007	0.000	0.001	4.345
2	As	0.0	0.0	0.0	-0.007	0.000	0.000	0.549
3	Mn	0.5	0.5	0.3536	3.879	0.000	0.000	10.091
4	As	0.5	0.5	0.7071	3.791	0.000	-0.006	10.079
5	Ga	1.0	1.0	1.0607	-0.020	0.000	0.000	0.587
6	As	0.0	0.0	1.4142	-0.021	0.000	0.000	0.585
7	Ga	0.5	0.5	1.7678	0.003	0.000	0.001	8.708
8	As	0.5	0.5	2.1213	-0.001	0.000	0.001	8.708
9	Ga	1.0	1.0	2.4749	0.003	0.000	0.000	0.564
10	As	0.0	0.0	2.8284	-0.001	0.000	0.001	0.567
11	Mn	0.5	0.5	3.1820	0.003	0.000	0.000	8.712
12	As	0.5	0.5	3.5355	0.001	0.000	0.000	8.711
13	Ga	1.0	1.0	3.8891	0.003	0.000	0.000	0.564
14	Fe	1.0	1.0	4.2426	0.000	0.000	0.000	0.565
					0.006	0.000	0.000	8.710
					0.004	0.000	0.000	8.710
					0.004	0.000	0.000	0.563
					0.003	0.000	0.000	0.562
					4.038	0.000	-0.002	10.090
					3.814	0.000	0.003	10.100
					-0.013	0.000	0.000	0.583
					-0.017	0.000	0.000	0.582
					0.018	0.000	0.000	8.696
					0.002	0.000	0.000	8.692
					1.531	0.000	0.008	4.363
					0.711	0.000	0.008	4.602

The calculated local magnetic moment lies on the x -axis and is ca. $4.0\mu_B$ for the multilayer and ca. $3.8\mu_B$ for the heterostructure. These results are in good agreement with the magnetic moment of $5\mu_B$ for free Mn atoms, which is reduced in the lattice since Mn acts as an acceptor. Larger differences appear for the magnetic moments of Fe atoms, which are surface atoms for the multilayer (ca. 1.0 and $1.5\mu_B$) and sub-monolayers for the superlattice (ca. $0.7\mu_B$). The atomic charges are very close for both structures. These results suggest that Mn dopants dominate the magnetic properties of the studied systems, but Fe atomic planes can be considered to be good metallic contacts in the case of multilayers.

In the next step, we performed spin polarized GGA calculations to evaluate the influence of Fe impurities on the electronic structure of the $\text{Ga}_{0.5}\text{Mn}_{0.5}\text{As}/\text{AsGa}/\text{Ga}_{0.5}\text{Mn}_{0.5}\text{As}/\text{Fe}$ heterostructure as compared to the $\text{Ga}_{0.5}\text{Mn}_{0.5}\text{As}/\text{AsGa}/\text{Ga}_{0.5}\text{Mn}_{0.5}\text{As}$ superlattice. The band structure calculated for that heterostructure seems to confirm the results described in Ref. [11], and the band dispersion in the direction perpendicular to the MnAs plane normal is very narrow, suggesting a two-dimensional electron transport system with small hopping between MnAs planes. The main results of the calculations are the densities of states (DOS) in the total and partial figure, projected onto ferromagnetic Mn and Fe atoms and 3d states for majority and minority spins.

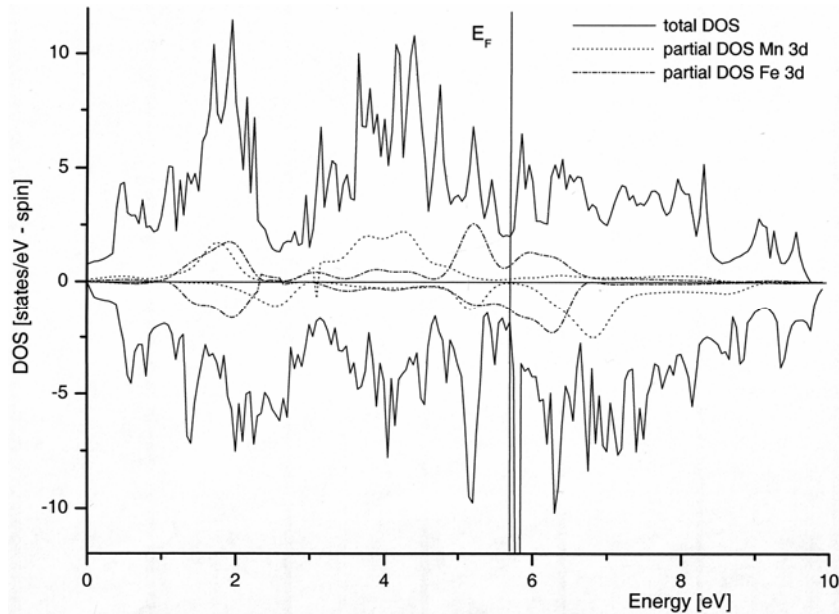


Fig. 1. Total DOS and partial DOS projected onto the Mn/Fe 3d states of the $\text{Ga}_{0.5}\text{Mn}_{0.5}\text{As}/\text{AsGa}/\text{Ga}_{0.5}\text{Mn}_{0.5}\text{As}/\text{Fe}$ heterostructure for the majority and minority spin channel

In the $\text{Ga}_{0.5}\text{Mn}_{0.5}\text{As}/\text{AsGa}/\text{Ga}_{0.5}\text{Mn}_{0.5}\text{As}/\text{Fe}$ superlattice (Fig. 1), both majority and minority total DOSs are nonzero at the Fermi energy level and the system has DOS features typical of ferromagnetic metals. Although the minority partial DOS for Mn

3d states is zero at the Fermi level, half-metallicity is destroyed by Fe 3d states at the Fermi level.

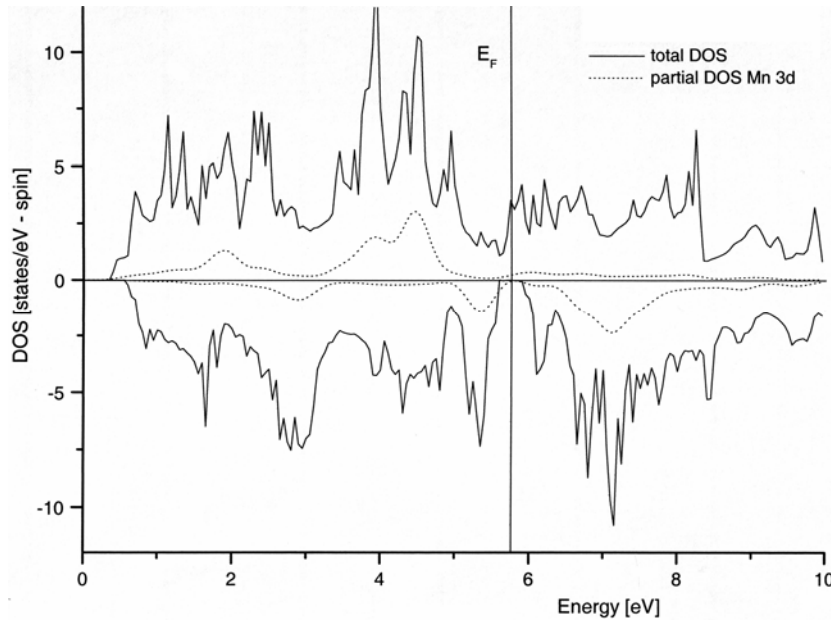


Fig. 2. Total DOS and partial DOS projected onto the Mn 3d states of the $\text{Ga}_{0.5}\text{Mn}_{0.5}\text{As}/\text{AsGa}/\text{Ga}_{0.5}\text{Mn}_{0.5}\text{As}$ superlattice for both majority and minority spin

It can be seen in Fig. 2 that the minority spin DOS at E_F has a small semiconductor gap of ca. 0.3 eV, but no such gap exists in the majority spin channel in the case of the $\text{Ga}_{0.5}\text{Mn}_{0.5}\text{As}/\text{AsGa}/\text{Ga}_{0.5}\text{Mn}_{0.5}\text{As}$ digital alloy. The mechanism of ferromagnetism for MnAs/GaAs digital alloys remains unclear in general [9], partly because of the large range of hole concentrations and the complexity of Mn/carrier interactions [18]. The metallic majority spin DOS at E_F is composed largely of As p states, suggesting that hole doping at the top of the valence band by Mn^{2+} 3d ions, and subsequent polarization of mobile charge carriers by interaction with exchange split energy levels Mn 3d, is responsible for the half-metallicity in this case.

4. Summary

In this article we have studied the electronic and magnetic properties of thin zinc blende superlattices with ferromagnetic dopants by DFT methods based on ultrasoft pseudopotentials. These fast DFT ultrasoft pseudopotential calculations can be competitive and complementary to relatively slow all-electron DFT calculations [19]. The DFT non-collinear magnetism technique exactly shows the magnetization localized on supercell atoms in Fe/MnAs/AsGa(0,0,1) multilayers and MnAs/AsGa(0,0,1) super-

lattices. These calculations are in good agreement with spin polarized GGA calculations for the studied zinc blende heterostructures. We suggest that Fe submonolayers in these systems can destroy the half-metallicity of MnAs/AsGa digital alloys.

In summary, we have shown that DFT *ab initio* calculations lead to a correct description of the magnetic and electronic properties and can be used to theoretically identify half-metallicity in zinc blende superlattices with ferromagnetic dopants and other spintronic materials.

References

- [1] ŽUTIĆ I., FABIAN J., DAS SARMA S., *Rev. Mod. Phys.*, 76 (2004), 323.
- [2] OHNO Y., YOUNG D.K., BESCHOTEN B., MATSKURA F., OHNO H., AWSCHALOM D.D., *Nature*, 402 (1999), 790.
- [3] FIEDERLING R., KEIM M., REUSCHER G., OSSAU W., SCHMIDT G., WANG A., MOLENKAMP L.W., *Nature*, 402 (1999), 787.
- [4] DATA S., DAS B., *Appl. Phys. Lett.*, 56 (1990), 665.
- [5] PRINZ G., *Science*, 282 (1998), 1660.
- [6] BURKARD G., LOSS D., DIVINCENZO D.P., *Phys. Rev. B*, 59 (1999), 2070.
- [7] KAWAKAMI R.K., JOHNSON-HALPERIN E., CHEN L.F., HANSON M., GUEBELS N., SPECK J.S., GOSSARD A.C., AWSCHALOM D.D., *App. Phys. Lett.*, 77 (2000), 2379.
- [8] DIETL T., OHNO H., MATSUKURA F., CIBERT J., FERRAN D., *Science*, 287 (2000), 1019.
- [9] SANVITO S., HILL N.A., *Phys. Rev. Lett.*, 87 (2001), 267202.
- [10] QIAN M.C., FONG C.Y., PICKETT W.E., PASK J.E., YANG L.H., DAG S., *Phys. Rev. B*, 71 (2005), 012414.
- [11] SANVITO S., *Phys. Rev. B*, 68 (2003), 054425.
- [12] GEBAUER R., BARONI S., *Phys. Rev. B*, 61 (2000), R6459.
- [13] BARONI S., DE GIRONNOLI S., DAL CORSO A., GIANNOZI P., *Rev. Mod. Phys.*, 73 (2001), 515.
- [14] VANDERBILT D., *Phys. Rev. B*, 41 (1990), 7892.
- [15] HOHENBERG P., KOHN W., *Phys. Rev.*, 136 (1964), B864.
- [16] PERDEW J.P., BURKE K., ERNZERHOF M., *Phys. Rev. Lett.*, 77 (1996), 3865.
- [17] MONKHORST H.J., PACK J.D., *Phys. Rev. B*, 13 (1976), 5188.
- [18] KAMINSKI A., DAS SARMA S., *Phys. Rev. Lett.*, 88 (2002), 247202.
- [19] WRONKA A., *Acta Physicae Superficerum*, 7 (2004), 111.

Received 1 June 2005
Revised 10 October 2005